JOURNAL OF THERMOPHYSICS AND HEAT TRANSFER
Vol. 19, No. 4, October–December 2005

Direct, Continuous Condensation of Steam in Flowing Water

Jim A. Clark* and Ryan W. Brandt†
Pratt & Whitney Space Propulsion, West Palm Beach, Florida 33410-9600

In some liquid-propellant rocket engines, the liquid-oxygen (LOX) boost pump is driven by a turbine that is powered by high-pressure gaseous oxygen. Once it exits the turbine, this gaseous oxygen can be salvaged by injecting it into the subcooled LOX exiting the boost pump. If the main LOX pump is to function correctly under these circumstances, complete condensation of the gaseous oxygen must quickly follow its injection into the boost-pump discharge. The current investigation uses steam and water in a simple rig that allows the condensation process to be visualized and quantified. This paper offers dimensionless-parameter correlations of the data and trends observed.

Nomenclature

$c_{p,\mathrm{liq}}$	=	average specific heat of liquid during condensation process
h_{liq}	=	enthalpy of liquid water approaching vapor-injection port
h_{vapor}	=	enthalpy of steam being injected
$\dot{m}_{\mathrm{liq}}$	=	mass flow rate of liquid water approaching vapor-injection port
$\dot{m}_{\mathrm{vapor}}$	=	mass flow rate of steam
T_{boil}	=	boiling temperature of the liquid at the pressure in the liquid tube, near the vapor-injection port
T_{liq}	=	temperature of liquid before it reaches the vapor-injection port
T_{mix}	=	calculated temperature of water after all steam has been condensed, $T_{\mathrm{liq}} + (\dot{m}_{\mathrm{vapor}} * h_{\mathrm{vapor}} + \dot{m}_{\mathrm{liq}} * h_{\mathrm{liq}})/(\dot{m}_{\mathrm{liq}} * c_{p,\mathrm{liq}})$
T_{mixratio}	=	T_{mix} (absolute temperature) divided by T_{boil} (absolute temperature)
T_{thresh}	=	the value of T_{mix} at which dimensionless condensation distance = 1.0
$T_{\mathrm{threshratio}}$	=	T_{thresh} (absolute temperature) divided by T_{boil} (absolute temperature)

I. Introduction

In liquid-propellant rocket engines, a boost pump is sometimes used to raise propellant pressure to a level that is well above the propellant's saturation pressure yet well below the final pressure that is produced in the main pump. This arrangement allows the propellant storage tank to operate at low pressure, it allows the boost pump to be optimized for suction performance, and it allows the main pump to be optimized for efficiency and packaging without compromise related to cavitation. To power a liquid-oxygen boost pump, a turbine driven by gaseous oxygen can be used, and the gaseous oxygen can be recovered by injecting it into the liquid oxygen emerging from the boost pump. The result of this injection is the condensation of the gaseous oxygen in the liquid oxygen being discharged from the boost pump.

In the condensation-based recovery of gaseous propellant in a boost turbopump, it is vital that the condensation process be complete before the liquid stream enters the main pump. The persistence of vapor bubbles in the liquid stream at the main-pump entrance can adversely affect main-pump performance. To quantify the distance needed to completely condense turbine exhaust gas under various operating conditions, the current investigation attempted to experimentally simulate turbine exhaust-gas recovery by condensation in a flowing liquid stream. In the current investigation, steam was a simulant for the turbine exhaust gas, and liquid water was a simulant for the liquid propellant that is discharged from a boost pump.

Presented as Paper 2004-4003 at the Joint Propulsion Conference, Fort Lauderdale, FL, 12–14 July 2004; received 19 October 2004; revision received 9 December 2004; accepted for publication 9 December 2004.

*Manager, Aerothermal Group, MS 713-31.
†Engineer, Aerothermal Group, MS 713-31.

II. Previous Research

Past research into the direct condensation of a vapor into a liquid had one of two focuses: the collapse of individual vapor bubbles in a pool of liquid, or the condensation rate of a vapor volume immediately above a reservoir of subcooled liquid. Regarding the study of individual vapor bubbles, multiple investigators[1–4] reported that bubble collapse was controlled by pressure differential (liquid pressure minus vapor pressure), bubble diameter, vapor density, and heat of vaporization. They also indicated that fluid motion at the liquid–vapor interface was an accelerator for the condensation process. Several other investigators[5–15] examined vapor condensation inside liquid-propellant tanks, indicating that condensation rate is greatly enhanced when mixing (generated by a submerged liquid jet, for example) promotes turbulence at the free surface of the liquid. Some of these investigations were concerned with tank-pressure control during tank-filling operations with cryogens in a low- or zero-gravity environment. Among these investigations, the experimental studies used either vapor and liquid water or vapor and liquid Freon.

The current investigation differed from these predecessors in several ways. First, the current experimental study did not use a pool or a reservoir of liquid. Instead, the liquid was flowing turbulently through a tube. Second, the current work was focused on a continuous-flow vapor stream entering perpendicularly to a flowing liquid stream. Third, because the current work involved flowing systems driven by significant pressure gradients, gravitational effects were negligible.

III. Experimental Apparatus

For safety and availability reasons, saturated steam and liquid water were used in the current experimental study. Figure 1 is a sketch of the test rig. Warm water in a reservoir was circulated by a two-stage, constant-speed centrifugal pump through a 9.5-mm-i.d. tubing circuit that began and ended at the reservoir. Liquid flow rate through the circuit was controlled by a valve in the bypass loop, which allowed some pump-discharge water to return to the pump inlet. Downstream of the pump, a turbine flow meter measured liquid flow rate, a thermocouple measured water temperature prior to the water's mixing with steam, and a transducer measured pressure in the mixing section. The steam-injection section of the circuit was a custom-made tee, such that the steam entered perpendicularly to the flowing water, whose path through the tee was straight. Clear polycarbonate tubing downstream of the tee allowed visualization

and measurement of the location of the condensation-process termination, which was marked by an abrupt change in the transparency of the liquid stream. In other words, wherever the liquid contained vapor bubbles, it was cloudy; wherever the vapor bubbles had all condensed, the liquid was clear. Downstream of the transparent tubing, a valve was available to control pressure in the mixing section. Finally, the liquid water, whose temperature had been increased by the injected steam, was returned to the reservoir. Reservoir temperature was controlled by continuous addition of cool water to the reservoir. This addition produced a continuous discharge of warm reservoir water through an overflow tube. Upstream of the mixing tee, saturated-steam flow rate was measured using the pressure drop across an orifice that had been previously calibrated with saturated steam.

In the current tests, liquid-water flow rates ranged from 0.027 to 0.082 m^3/min, liquid-water temperatures ranged from 294 to 364 K, steam flow rates ranged from 0.0023 to 0.0095 kg per second, and mixing-section pressures ranged from 1.8 to 3.1 atm absolute. Although the water pump was capable of producing higher pressures, the steam-supply pressure was limited to 4.4 atm absolute. Thus, operating the mixing section at pressures above 3.1 atm absolute would have produced unacceptably low steam flow rates. Throughout all tests described in this paper, the liquid-tube inner diameter (9.5 mm) remained constant; the steam-injection-port diameter was either 6.3 or 3.2 mm in all tests. Approaching the vapor-injection port, liquid Reynolds numbers ranged from 9×10^4 to 4×10^5.

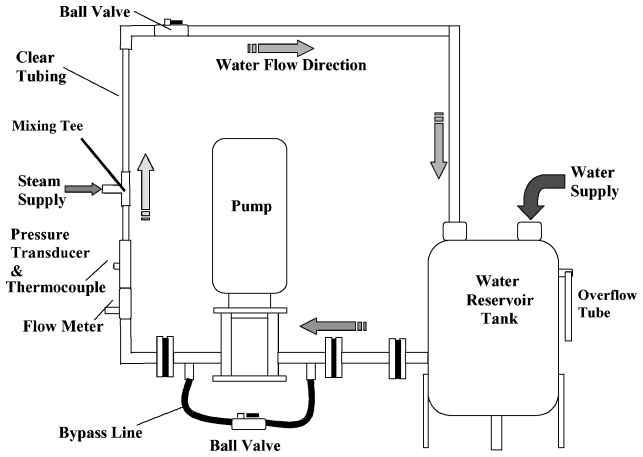

Fig. 1 Schematic of rig for measuring steam condensation in flowing water.

IV. Discussion of Results

During a typical test with water circulating and steam flowing, the externally supplied cool-water flow rate into the reservoir was adjusted to allow a very slow rate of water temperature rise entering the pump. At low water temperatures, the steam-condensation distance was too small to measure. As the water warmed, the distance for complete steam condensation increased, allowing steam-condensation distance, water temperature, water pressure, water flow rate, steam flow rate, steam pressure, and steam temperature to be recorded at each of several specific condensation distances. Once the water temperature had risen to the point where complete condensation required a distance longer than what could be measured through the clear polycarbonate tubing, the test was terminated and the reservoir was emptied and refilled with cool water in preparation for another test with a different combination of steam and water flow rates.

Figure 2 shows test data for a constant steam flow rate and a constant water flow rate. Steam-condensation distance (measured from the steam-injection-port axis to the condensation-completion point, by eye, using a scale) has been normalized by steam-injection port diameter and called dimensionless condensation distance (DCD) because in general, the larger the steam jet, the longer the steam survives before the jet disintegrates and the condensation process is complete. Liquid temperatures (after mixing with steam) have been normalized by boiling-point temperature ($T_{\text{mixratio}} = T_{\text{mix}}/T_{\text{boil}}$) to account for the observation that mixed-temperature proximity to boiling temperature is a better indicator of condensation performance than the liquid temperature alone. In presenting these data, Jakob number would have been a suitable substitute for T_{mixratio}, except that the traditional definition of Jakob number does not include the effects of vapor superheat and variable liquid specific heat. In contrast, T_{mix}, the enthalpy-based calculated temperature of the liquid after all steam has been condensed, includes both effects. Otherwise, the difference between Jakob number and T_{mixratio} is purely algebraic; as liquid water approaches its boiling temperature, T_{mixratio} approaches 1.0, and Jakob number approaches 0.0. Note in Fig. 2 that an equation of the form

$$\text{DCD} = \exp[C1 * (T_{\text{mixratio}} - T_{\text{threshratio}})] \tag{1}$$

where $C1$ is a constant, fits the data well. In this figure, the value of $T_{\text{threshratio}}$ is 0.808, implying that, for this geometry and this combination of steam and water flow rates, the condensation distance is negligibly small if T_{mix} is less than or equal to 80% of the boiling temperature, using an absolute temperature scale. This implication is consistent with the investigators' experience: when flowing water temperatures are relatively cool, steam condenses immediately.

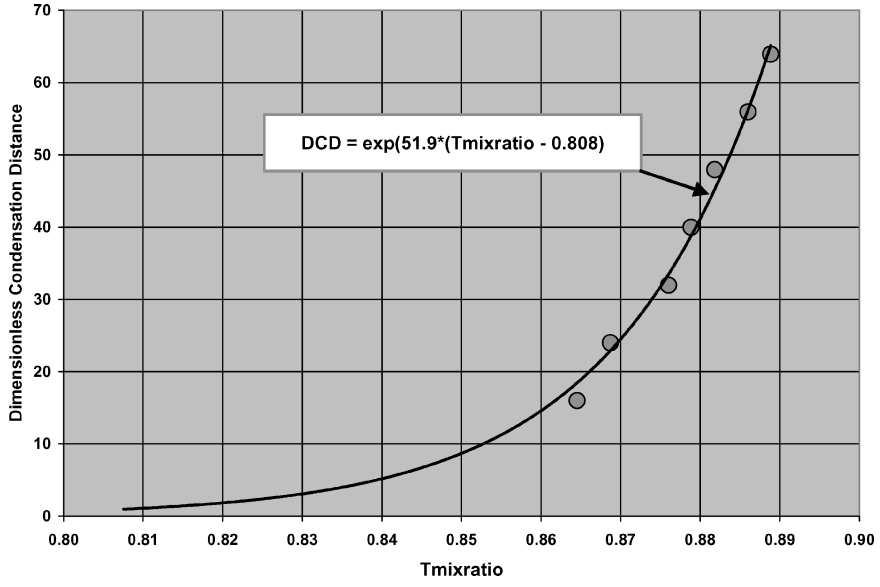

Fig. 2 DCD vs T_{mixratio} for DiamRatio = 0.33, MomRatio = 0.77.

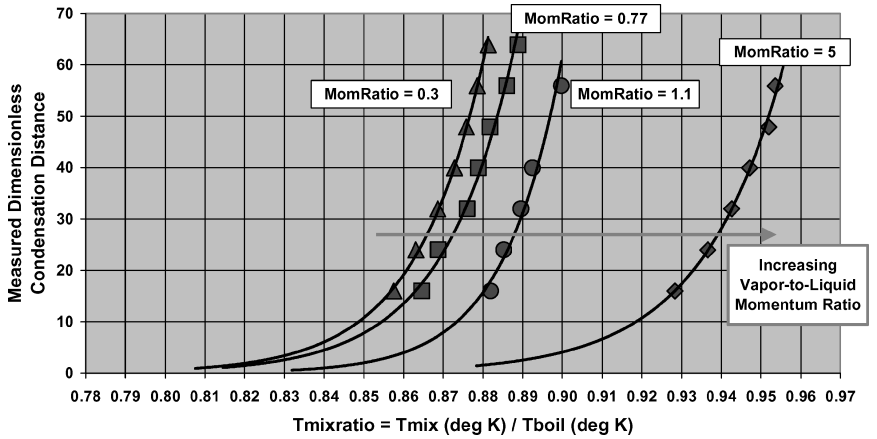

Fig. 3 Dimensionless condensation distance vs T_{mixratio} for DiamRatio = 0.33; 0.3 < MomRatio < 5.6.

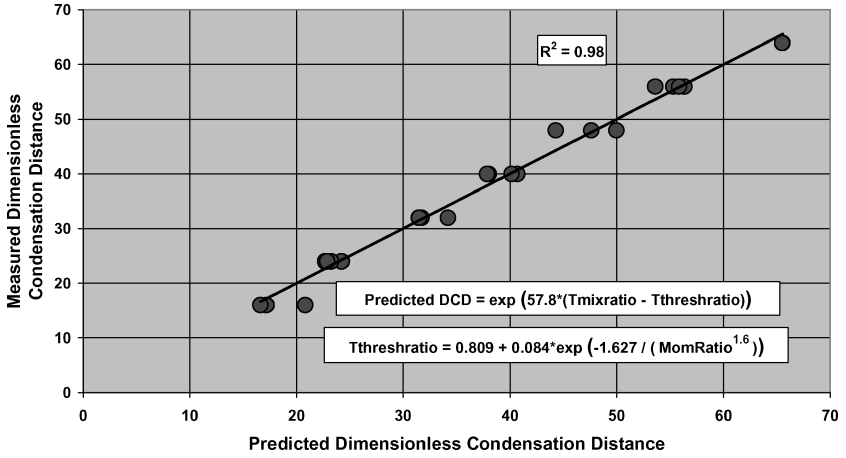

Fig. 4 Correlation of dimensionless condensation distances for DiamRatio = 0.33.

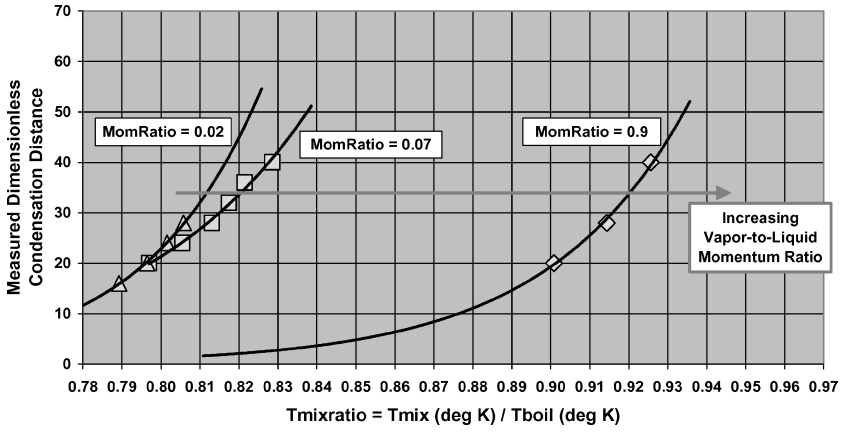

Fig. 5 DCD vs T_{mixratio} for DiamRatio = 0.67; 0.02 < MomRatio < 0.9.

Figure 3 is a plot of all dimensionless condensation data for vapor-injection-port diameter divided by the liquid-tube diameter (DiamRatio) = 0.33. Note in Fig. 3 that the vapor-injection momentum divided by the liquid momentum (MomRatio) ranged from 0.3 to 5, and that the average value of T_{mixratio} is higher when MomRatio is higher. High values of MomRatio promote rapid liquid-vapor mixing, which means that condensation can be quickly accomplished even when T_{mix} is near the boiling point. The trends of Fig. 3 indicate that dimensionless condensation data with MomRatio lower than 0.3 would fall only slightly to the left of the data that are already in Fig. 3. Similarly, Fig. 3 indicates that dimensionless condensation data with MomRatio greater than 5 would fall only slightly to the right of the data that are already in Fig. 3, because by definition, condensation cannot occur when T_{mixratio} is greater than or equal to one. Thus, for DiamRatio = 0.33, it is reasonable to assume that there is an upper bound and a lower bound for the values of $T_{\text{threshratio}}$. Specifically, the $T_{\text{threshratio}}$ lower bound appears to be close to 0.8, and the $T_{\text{threshratio}}$ upper bound appears to be close to 0.9. Therefore, an equation that appears to describe the influence of MomRatio on $T_{\text{threshratio}}$ is of the form

$$T_{\text{threshratio}} = C2 + C3 * \exp(-C4/\text{MomRatio}^{C5}) \qquad (2)$$

where $C2$ is the lower bound, the sum $C2 + C3$ is the upper bound for $T_{\text{threshratio}}$ and $C5$ is an exponent larger than positive one. Figure 4 is a correlation, employing Eqs. (1), and (2), of all dimensionless-condensation data for DiamRatio = 0.33.

Figure 5 is a plot of all dimensionless-condensation data for DiamRatio = 0.67. Again, the higher the MomRatio, the higher the

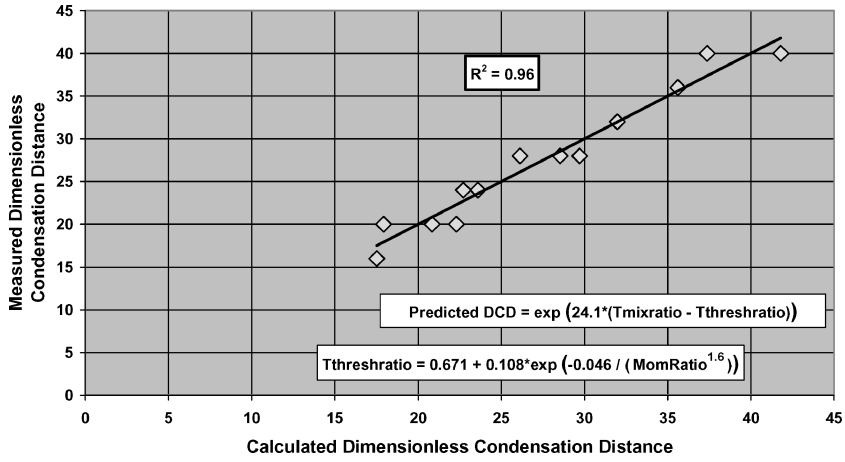

Fig. 6 Correlation of DCDs for DiamRatio = 0.67.

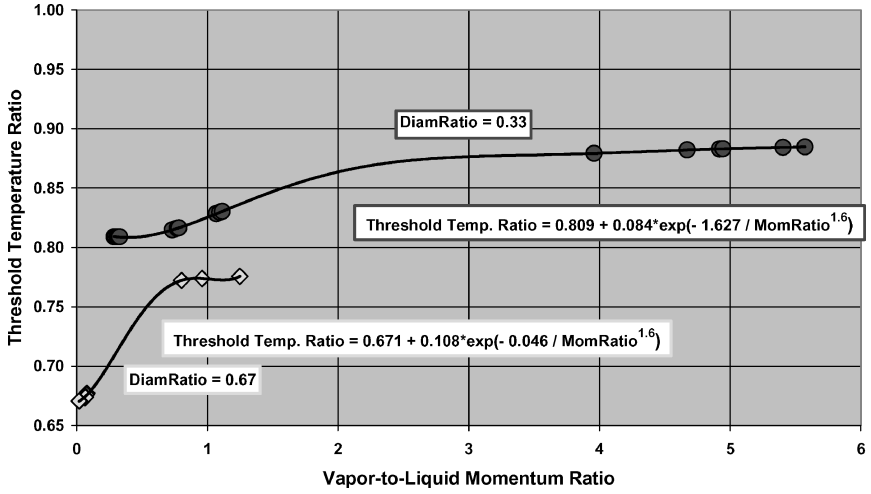

Fig. 7 The effect of MomRatio and DiamRatio on $T_{\text{threshratio}}$.

$T_{\text{threshratio}}$. Figure 6 is a correlation, employing Eqs. (1) and (2), of all dimensionless-condensation data for DiamRatio = 0.67.

Figure 7 illustrates how $T_{\text{threshratio}}$ depends on MomRatio and DiamRatio. In the current study, the higher value of DiamRatio is generally associated with lower values of $T_{\text{threshratio}}$; that is, when the steam-injector port is larger, colder water is needed to produce immediate condensation of all steam. Higher values of MomRatio are associated with higher values of $T_{\text{threshratio}}$, but MomRatio values above 3 appear to have no additional effect on $T_{\text{threshratio}}$.

Figure 7 suggests that a single equation involving MomRatio and DiamRatio might be used to predict $T_{\text{threshratio}}$. That equation could take the form

$$T_{\text{threshratio}} = (A1 + A2 * \text{DiamRatio}) + A3 * [1 - \exp(A4 * \text{DiamRatio})] * \exp[(A5 + A6 * \text{DiamRatio})/\text{MomRatio}^{1.6}] \quad (3)$$

where $C2$ in Eq. (2) has been replaced by $(A1 + A2 * \text{DiamRatio})$ in Eq. (3). Also, $C3$ in Eq. (2) has been replaced by $A3 * [1 - \exp(A4 * \text{DiamRatio})]$ in Eq. (3), and C4 in Eq. (2) has been replaced by $(A5 + A6 * \text{DiamRatio})$ in Eq. (3). The forms of these substitutions were chosen to allow calculation of reasonable values of $T_{\text{threshratio}}$ for MomRatio from 0 to 6 and for DiamRatio from 0 to 0.67.

After the same fashion, Figs. 4 and 6 suggest that a single equation involving DiamRatio, T_{mixratio}, and $T_{\text{threshratio}}$ can be used to predict DCD. That equation has the form

$$\text{DCD} = \exp[(A7 + A8 * \text{DiamRatio}) * (T_{\text{mixratio}} - T_{\text{threshratio}})] \quad (4)$$

Figure 8 is the final overall correlation of all dimensionless condensation data using Eqs. (3) and (4).

A legitimate criticism of the correlation in Fig. 8 is that it relies on too many fitting constants to achieve a high correlation coefficient. The authors acknowledge this aspect of the correlation. However, in several ways, the form of the correlation is sensible. For example, in Eq. (4), the rate of rise of the exponential term would be expected to vary with DiamRatio, because vapor-jet diameter affects the rate of mixing, which affects condensation distance. Similarly, in Eq. (3), the minimum value of $T_{\text{threshratio}}$, that is, the value of $T_{\text{threshratio}}$ when MomRatio is near zero, should reasonably be expected to depend on DiamRatio. When the vapor-jet diameter is larger, colder liquid is needed for instant condensation of all of the vapor. Finally, the magnitude of the effect of MomRatio on $T_{\text{threshratio}}$ should be expected to depend on $T_{\text{threshratio}}$. When $T_{\text{threshratio}}$ is not close to 1, then increasing the MomRatio can raise $T_{\text{threshratio}}$ by 0.1 or more. However, when $T_{\text{threshratio}}$ is above 0.9, then increasing the MomRatio must by definition raise $T_{\text{threshratio}}$ by less than 0.1 to conform to the requirement that $T_{\text{threshratio}}$ must always remain below 1.0.

Although Eqs. (3) and (4) (on Fig. 8) produce reasonable values of DCD when DiamRatio is in the range from 0.0 to 0.67, the extrapolation of Eqs. (3) and (4) for values of DiamRatio significantly above 0.67 is problematic. The Eq. (3) linear substitution for $C2$ in Eq. (2) indicates that the minimum value of $T_{\text{threshratio}}$ should be equal to 0.54 when the DiamRatio equals 1. However, the investigators' brief experimentation with a geometry involving DiamRatio = 1 (not reported here) indicates that $T_{\text{threshratio}}$ values for DiamRatio = 1.0 are in the same range as the $T_{\text{threshratio}}$ values for a DiamRatio = 0.67, probably because of the blockage presented by a steam jet whose diameter is equal to the liquid-stream diameter. In this

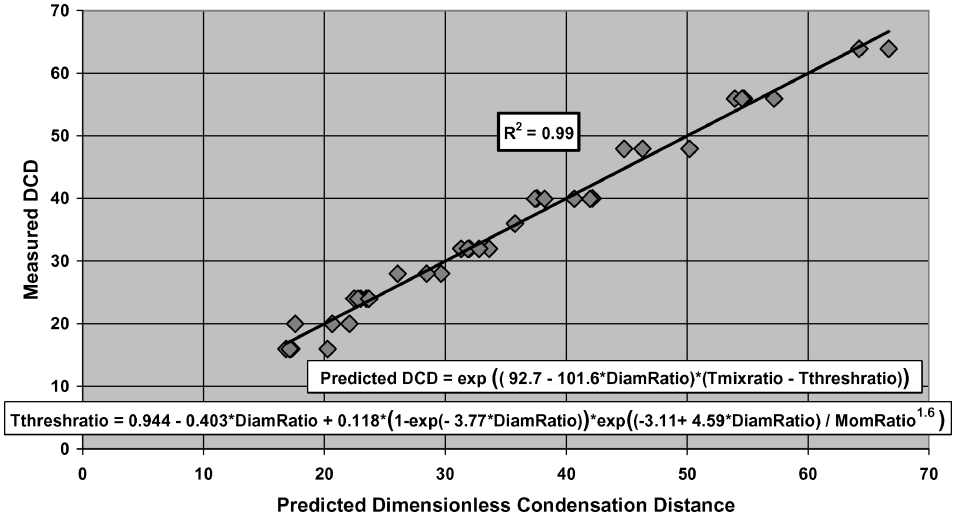

Fig. 8 Overall correlation for DCD of a single vapor jet in flowing liquid.

situation, the liquid stream does not have the option of flowing around the vapor jet. Instead, the liquid stream is forced to penetrate and vigorously mix with the vapor jet. Thus, the extrapolation of Eqs. (3) and (4) for values of DiamRatio greater than 0.67 is not recommended, although such extrapolation may be safe for values of MomRatio less than 0.1, that is, when the vapor jet does not significantly block the liquid stream.

V. Conclusions

This paper has presented dimensionless condensation distances for single-port, perpendicular, continuous injection of steam into turbulent, flowing liquid water. Condensation distances have been shown to depend on vapor-port diameter, MomRatio, DiamRatio, and T_{mixratio}. As expected, the lower the value of T_{mixratio} and the smaller the vapor-port diameter, the shorter the condensation distance. Also, elevated values of MomRatio promote mixing, which shortens condensation distance.

The effect of DiamRatio is more complex. At low MomRatio (less than 0.5), mixing is minimized, and the condensation process is made less efficient by DiamRatio increases. At high MomRatio (greater than 0.5), a larger-diameter vapor jet's increased penetration of the liquid stream promotes mixing, thereby accelerating the condensation process and partially offsetting the longer condensation length typically associated with a larger-diameter jet.

Nearly instantaneous condensation appears achievable if the value of T_{mixratio} is kept below 0.6, regardless of MomRatio or DiamRatio. This finding indicates that the influences of vapor-injection geometry and momentum may be muted by keeping T_{mixratio} low. However, even at T_{mixratio} values greater than 0.6, instantaneous condensation can also be achieved with a small vapor port in combination with a MomRatio above 2.

To fully understand the physics of continuous-flow vapor condensation in a flowing liquid stream, more experimental work is needed. For single-port vapor injection, condensation distances need to be measured for DiamRatio >0.67, and for vapor injection that is not perpendicular to the liquid stream. Furthermore, multiport vapor injection should be explored. At first glance, multiport vapor injection seems like a scheme that can minimize vapor-condensation distance, because the size of each vapor-injection port is smaller than it would be for a single port with the same total port area. However, at low MomRatio, multiport vapor injection may worsen condensation performance because small vapor jets do not penetrate a liquid stream as far as a larger, single jet of the same flow rate and MomRatio. In addition, the port-to-port spacing and orientation of a multiport injection scheme may significantly impact the condensation process; vapor ports that are in line with one another or too close to one another may inhibit mixing between the liquid and the vapor. Finally, for condensation tests with either single-port or multiport vapor injection, use of superheated vapor or a vapor/liquid combination other than steam/water is desirable, to learn whether the correlations developed in the current effort apply to such situations.

Acknowledgments

NASA sponsored this work under contract NAS8-01108. The authors thank Brian Goode of NASA Marshall Space Flight Center for his consultation and advice during the test program. The authors also thank Charles Whipple of Pratt & Whitney Space Propulsion for developing the steam-condensation rig described in this paper.

References

[1]Florschuetz, L. W., and Chao, B. T., "One the Mechanics of Vapor Bubble Collapse," *Journal of Heat Transfer*, May 1965, pp. 209–220.

[2]Wittke, D. D., and Chao, B. T., "Collapse of Vapor Bubbles with Translatory Motion," *Journal of Heat Transfer*, Feb. 1967, pp. 17–24.

[3]Hao, Y., and Prosperetti, A., "The Collapse of Vapor Bubbles in a Spatially Non-uniform Flow," *International Journal of Heat and Mass Transfer*, Vol. 43, 2000, pp. 3539–3550.

[4]Levenspiel, O., "Collapse of Steam Bubbles in Water," *Bubble Dynamics*, Vol. 51, No. 6, 1959, pp. 787–790.

[5]Dominick, S. M., "Mixing Induced Condensation Inside Propellant Tanks," AIAA Paper 1984-514, 1984.

[6]Helmick, M. R., Khoo, B. C., Brown, J. S., and Sonin, A. A., "Vapor Condensation Rate at a Turbulent-Liquid Interface for Application to Cryogenic Hydrogen," AIAA Paper 1988-559, 1988.

[7]Brown, J. S., Helmick, M. R., and Sonin, A. A., "Vapor Condensation at a Turbulent Liquid Surface in Systems with Possible Space-Based Applications," AIAA Paper 1989-2846, 1989.

[8]Lin, C.-S., "Numerical Studies of the Effects of Jet-Induced Mixing on Liquid-Vapor Interface Condensation," AIAA Paper 1989-1744, 1989.

[9]Vaughan, D. A., and Schmidt, G. R., "Analytical Modelling of No-Vent Fill Process," AIAA Paper 1990-2377, 1990.

[10]Lin, C.-S., and Hasan, M. M., "Vapor Condensation on Liquid Surface Due to Laminar Jet-Induced Mixing: The Effects of System Parameters," AIAA Paper 1990-0354, 1990.

[11]Jones, O. S., Meserole, J. S., and Bentz, M. D., "Correlation of Ullage Condensation Rate with Mixing Intensity in Propellant Tanks," AIAA Paper 1991-2543, 1991.

[12]Lin, C. S., and Hasan, M. M., "Vapor-Condensation on Liquid Surface due to Laminar Jet-Induced Mixing," *Journal of Thermophysics and Heat Transfer*, Vol. 5, No. 4, 1991, pp. 607–612.

[13]Schmidt, G. R., Carrigan, R. W., Hahs, J. E., Vaughan, D. A., and Foust, D. C., "No-Vent Fill Pressurization Test Using a Cryogen Simulant," AIAA Paper 1992-3062, 1992.

[14]Lin, C. S., Hasan, M. M., and Nyland, T. W., "Mixing and Transient Interface Condensation of a Liquid Hydrogen Tank," AIAA Paper 1993-1968, 1993.

[15]Lin, C. S., Hasan, M. M., and Van Dresar, N. T., "Experimental Investigation of Jet-Induced Mixing of a Large Liquid Hydrogen Storage Tank," AIAA Paper 1994-2079, 1994.